Corrosion Science 83 (2014) 67–74

Contents lists available at ScienceDirect

Corrosion Science

journal homepage: www.elsevier.com/locate/corsci

The effect of moisture content on the corrosion of fasteners embedded in wood subjected to alkaline copper quaternary treatment

Samuel L. Zelinka [a,*], Samuel V. Glass [a], Dominique Derome [b]

[a] Durability and Wood Protection Research, US Forest Service, Forest Products Laboratory 1 Gifford Pinchot Dr. Madison, WI 53726, USA
[b] Chair of Building Physics, Swiss Federal Institute of Technology in Zurich (ETHZ), CH-8093 Zürich, Hönggerberg, Switzerland

ARTICLE INFO

Article history:
Received 12 December 2013
Accepted 31 January 2014
Available online 8 February 2014

Keywords:
A. Steel
A. Zinc
B. Polarization
B. Weight loss
B. X-ray diffraction

ABSTRACT

This paper characterizes the corrosion rate of embedded fasteners as a function of wood moisture content using gravimetric and electrochemical measurements. The results indicated that the corrosion rate increased with moisture content before reaching a plateau. The phases present in the corrosion products, as analyzed using X-ray diffraction, are generally consistent with previous work. Uniform corrosion was observed for all fasteners and all conditions except steel fasteners embedded in water-saturated wood. Data of dependence of corrosion rate on moisture content, presented herein, are necessary to ensure the accuracy of combined hygrothermal/corrosion models used to predict durability of wood structures.
Published by Elsevier Ltd.

1. Introduction

Moisture plays an important role in the corrosion of metals in wood. Wood is a hygroscopic material and freely exchanges water with the environment, establishing an equilibrium moisture content (MC, defined as the ratio of the mass of water to the mass of dry wood, expressed either as a percentage or decimal) that depends upon the temperature and relative humidity of the ambient air, and also on its previous moisture history of the wood. Metal fasteners in wood can therefore be exposed to moisture conditions that could lead to corrosion [1–17]. However, when the wood moisture content is low, there may be a threshold moisture content below which fasteners do not corrode in wood [11,18–23]. The first work that suggested a threshold for corrosion was performed by Baechler [19,20] who examined the corrosion of fasteners in wood that was in equilibrium with air at 30% relative humidity (RH), 65% RH, 90% RH and an outdoor exposure. For untreated pine (*Pinus ponderosa*), the corrosion rate was zero for the 30% RH and 65% RH conditions, but jumped to 6 μm year^{-1} at 90% RH (approximately 20% MC) [24]. Baechler observed similar trends for wood treated with zinc chloride. Kear et al. measured the corrosion rate of steel and galvanized steel fasteners in untreated pine (*Pinus radiata*) and pine treated with chromated copper arsenate (CCA), alkaline copper quaternary (ACQ), and copper azole (CA) conditioned at 75% RH, 90% RH, and "moisture saturated air" [11]. Corrosion at 75% RH (approximately 14% MC) was nearly undetectable. These gravimetric tests suggest that corrosion of embedded metals begins to occur when wood is in equilibrium with a relative humidity of 70–75%. However, the data collected in these gravimetric tests are too sparse to understand how the corrosion rate changes above the threshold. Other researchers have used electrochemical test methods to better understand the role of moisture on metals corroding in wood.

Dennis et al. used polarization resistance measurements at many moisture contents to examine how the corrosion rate changes with moisture content in CCA treated wood [22]. A zinc coupon was used as a working electrode and was placed between two sections of treated wood, one side of which had a salt bridge to a reference electrode. The moisture content was lowered from near saturation to 15% MC by letting the wood air dry in a "semi-sealed container". It was then raised back to saturation by placing it in a 100% RH environment and removing it in intervals for measurement. Importantly, the wood was not allowed to reach equilibrium except near saturation and at 15% MC. We replot their data of the corrosion current density (which is proportional to the corrosion rate) as a function of moisture content in Fig. 1. The corrosion rate exhibits hysteresis when plotted against moisture content, which is not physically meaningful. This most likely arises from the fact that the wood was not in equilibrium when the measurements were taken. The corrosion rate has a sigmoidal dependence on moisture content with a threshold at 15% MC and a plateau above

* Corresponding author.
E-mail address: szelinka@fs.fed.us (S.L. Zelinka).

http://dx.doi.org/10.1016/j.corsci.2014.01.044
0010-938X/Published by Elsevier Ltd.

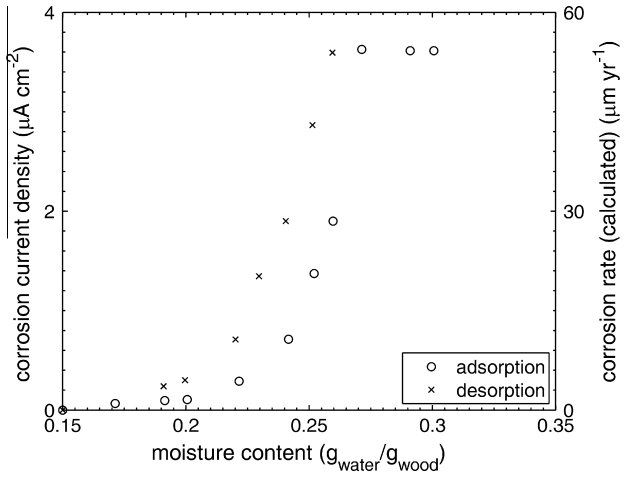

Fig. 1. Corrosion current density, as a function of wood moisture content as measured by Dennis et al. [6] for galvanized steel in contact with wood treated with CCA from polarization resistance measurements.

25% MC. These data are consistent with the observations from gravimetric tests; however, because of the number of conditions tested a more detailed curve could be developed.

The data of Dennis et al. [22] exhibit a sigmoidal dependence on moisture content. In general data with this shape can be fit by an equation of the form

$$R = \frac{A}{1 + \exp[B(C - M)]} \quad (1)$$

where the corrosion rate, R, depends upon the moisture content M, and A, B, and C are fitting parameters that represent the asymptotic maximum corrosion rate, the steepness of the transition from zero corrosion rate to the maximum, and the location of the transition, respectively. Zelinka et al. [25] have used Eq. (1) to predict the corrosion rate (R) of embedded fasteners as a function of moisture content (M). The parameters B and C describing the steepness and location of the transition were taken from a fit of the data of Dennis et al. [22]. The asymptotic corrosion rate at very high moisture content (A) was taken from corrosion rates measured electrochemically in water-extracts of treated wood, which were shown to have corrosion rates similar to those measured gravimetrically in solid wood exposed to 100% relative humidity [26–29]. Eq. (1) was implemented as a post-processor in a hygrothermal model; the hygrothermal model calculates the wood moisture content using hourly climatic data, and the post-processor calculates the amount of corrosion. The accuracy of this method is limited in part by the lack of data on the corrosion rate as a function of moisture content.

While previous studies have shown that the corrosion rate increases with moisture content up to a plateau (resulting from fiber saturation of the wood), it is unclear whether the mechanism of corrosion also changes with moisture content. The only work that examined the corrosion products of metals embedded in treated wood was performed by Zelinka et al. [27], who used X-ray diffraction to identify the corrosion products of fasteners embedded in wood exposed to 100% relative humidity. Under these conditions, the corrosion products that form on fasteners embedded in wood differ from those that form in atmospheric corrosion. These differences both affect the corrosion rate and relative performance of steel and galvanized steel fasteners [27]. For fasteners embedded in wood and exposed to a 100% relative humidity environment, smithsonite ($ZnCO_3$), the passivating, protective zinc corrosion product [30,31], did not form which resulted in the galvanized fasteners corroding more rapidly than steel fasteners [27]. It is not clear if the same corrosion products form at all moisture contents, or if this only occurs at 100% relative humidity.

This paper investigates the corrosion kinetics and corrosion products of fasteners embedded in wood through a combination of gravimetric and electrochemical measurements. One goal of the work is to develop more data that can be used in combined hygrothermal–corrosion modeling. The work builds upon previous studies that examined corrosion at different relative humidities [11,19,20] but extends into the over-hygroscopic region. In addition, the work adds to the very limited knowledge of the corrosion products that form on metals embedded in wood.

2. Methods and materials

Two complementary methods were used to evaluate the dependence of corrosion rates on wood moisture content: exposure tests, in which fasteners were embedded into wood and exposed at one of four moisture conditions for a year, and electrochemical tests, in which small metal coupons were held against the wood specimens and polarized. In addition, the corrosion products on the fasteners used in the exposure test were examined.

All wood specimens were cut from a single beam of southern pine, believed to be slash pine (*Pinus elliottii*). In the time between sawmilling and transit to the laboratory, the beam was partially infected with a blue stain fungus; whether blue stain has any effect on corrosion is unknown, but blue stain contamination is common in commercially available lumber. For the exposure test, wood specimens were cut along the anatomical planes of the wood to 38 mm (tangential) by 89 mm (radial) (nominal US "2 × 4") by 610 mm (longitudinal) and the fasteners were driven into a purely tangential face. The specimen size was chosen to correspond with the ASTM G198 standard [32]. The specimens used in the electrochemical test were cut into small 25 mm by 25 mm blocks with a thickness in the longitudinal direction of 9.5 mm. All wood specimens were treated with waterborne alkaline copper quaternary (type D) as specified in AWPA standard P5 [33]. The composition of the preservative consists of 66.7% copper oxide and 33.3% didecyldimethylammonium carbonate dissolved in ethanolamine. The treatment was performed by submersing the wood in a treatment solution, pulling a vacuum (20 kPa absolute pressure) for 30 min, followed by applying a pressure of 1034 kPa for 60 min. The targeted preservative retention was 4 kg of wood preservative m^{-3} of wood, which was the recommended preservative retention for above ground use [34] at the time this study was initiated; the calculated actual preservative retention based upon solution uptake was 3.5 kg m^{-3}. This preservative retention corresponds to approximately 1.9 kg of elemental copper m^{-3} of wood.

2.1. Exposure test

Four different moisture conditions were tested, all at 27 °C. The first two conditions were equilibrium conditions achieved by placing the wood specimens in environmental chambers maintained at 90% RH and 95% RH, respectively. The specimens were allowed to come to equilibrium prior to the driving of fasteners into the specimens. Wood moisture contents remained stable for each specimen throughout the test, and replicate specimens had roughly the same moisture contents. For the third condition, specimens were first equilibrated at 95% RH. Fasteners were then driven and specimens were placed in a desiccator above a reservoir of water (100% RH). These specimens had small differences in moisture content among replicates. The fourth condition was obtained by submerging end-sealed specimens under water for several days. Fasteners were then driven and wood specimens were placed in a sealed container in contact with a small amount of liquid water (100% RH). These

samples picked up a small amount of moisture during the test and remained above the fiber saturation point throughout the test. The corrosion rate was measured on nine galvanized and nine steel fasteners embedded in wood that was exposed to each condition; in total 72 different fasteners were examined that had been embedded in eight different pieces of wood.

Steel and hot-dip galvanized steel nails (8d, 3.4 mm in diameter 64 mm in length) were tested. The steel nails and galvanized nails came from the same production run; the steel nails were removed from the assembly line prior to galvanization. The surface areas of the nails were determined from high resolution digital images using the method of Rammer and Zelinka [35–37]. The coating thickness of the galvanized fasteners ranged between 10 and 25 μm. The compositions of the carbon steel nails and hot-dip galvanized coatings were analyzed by X-ray fluorescence. The carbon steel nail contained 0.73 wt.% Mn, 0.27 wt.% Cu, 0.16 wt.% Si, 0.15 wt.% Ni, 0.10 wt.% Cr, 0.04 wt.% Zn, and 0.01 wt.% Mo with the remainder as Fe. The surface of the galvanized coating contained 3.8 wt.% Fe, 1.7 wt.% Bi, 0.14 wt.% Pb, 0.12 wt.% Co, 0.06 wt.% Cr, 0.01 wt.% Ti, and 0.01 wt.% Zr with the balance as Zn. Immediately before being driven into the wood, the fasteners were cleaned in a three step process and weighed to the nearest 0.1 mg. The cleaning process consisted of ultrasonic cleaning for 5 min in a soap solution, following by a water rinse and 5 additional minutes of ultrasonic cleaning in a deionized water bath after which the fasteners were rinsed with acetone and allowed to dry.

After exposure, the fasteners were removed from the blocks of wood by sectioning along the 610 mm direction with the saw coming close to, but not in contact with the nails. This resulted in thin slices of wood that included the fasteners and thicker sections that came from the space between the fasteners. These thicker specimens were immediately sealed in a polyethylene bag until they could be weighed, after which they were oven-dried, and reweighed to determine the moisture content near each fastener. The nail could be removed from the thin section by hand without damaging the corrosion products. The loosely adhered corrosion products were removed and collected by lightly brushing the fasteners with a glass microscope slide. The fasteners were then cleaned in a 50:50 (volume ratio) mixture of water and Evpo-Rust™ (Orison Marketing, Abilene TX, USA) and weighed to determine mass loss, and thereby, the corrosion rate.

Collected corrosion products were analyzed and identified using powder X-ray diffraction. An Inel (Artenay, France) CPS 120 wide angle diffractometer with a Cu Kα source was used to collect the powder X-ray diffraction patterns.

2.2. Electrochemical test

The geometry of the electrochemical test is shown in Fig. 2 and consisted of sandwiching the 25 mm square wood block with a 50 mm by 25 mm by (thickness) galvanized coupon (working electrode) on one side and a 25 mm cube of graphite on the other side (counter electrode). Since only a 25 mm by 25 mm section of the working electrode was in contact with the "electrolyte" the effective area used in the calculation of the corrosion rate was taken as 625 mm^2. Preliminary measurements (data not shown) included a reference electrode; however it was not possible for the reference electrode to make sufficiently good contact to the solid wood to get a reliable reading. Since it was not possible to use a reference electrode, the lead for the reference electrode was connected to the counter electrode which resulted in all measurements being taken with respect to the open circuit potential. Pressure (4 MPa) was applied between the electrodes from a pneumatic cylinder and this pressure was chosen as it ensured good contact between the specimen and the electrodes. The pressure was chosen for several reasons. In preliminary measurements without any pressure, the measurements had higher variability and the polarization resistance was physically unreasonable (too high). Experiments performed with pressures above 4 MPa of pressure could not be statistically distinguished from those at 4 MPa. Finally, in other research that examined the relationship between contact pressure and the resistivity of wood showed that showed that contact effects were minimal above 1.5 MPa, but measurements at pressures from 4 to 14 MPa were nearly identical [38].

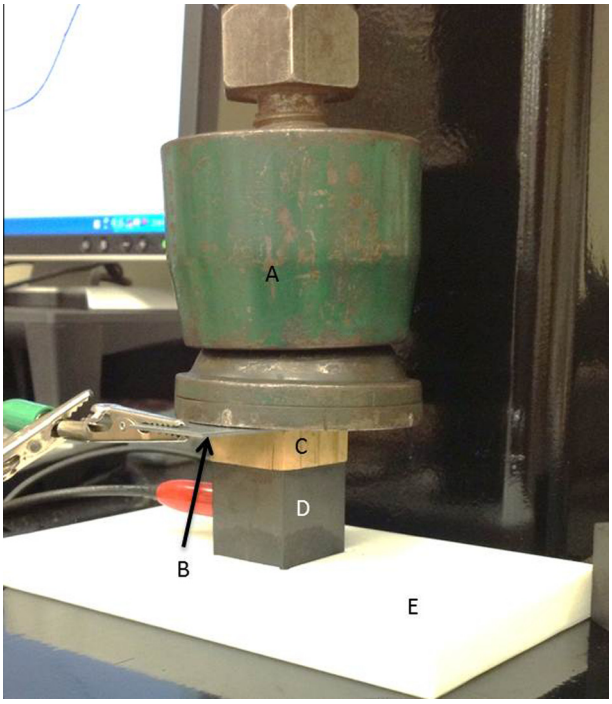

Fig. 2. Electrochemical test setup. Pressure (A) was applied to the working electrode (B) forcing it in contact with the wood specimen (C). A graphite counter electrode (D) was placed on the other side of the wood specimen and electrically isolated from the test setup by a PTFE block (E).

The corrosion rate was measured by the polarization resistance technique where the Tafel slopes were obtained from the nonlinearity in the potential vs. current curve using Mansfeld's method [39,40]. The system was polarized from −30 mV to +30 mV with respect to the open circuit potential at a scan rate of 0.167 mV s^{-1}. The average anodic Tafel slope was 80 mV per decade with a standard error of 6 mV per decade. The average cathodic Tafel slope was −57 mV per decade with a standard error of 3 mV per decade.

Since the DC electrical resistivity of wood changes by over 10 orders of magnitude from water saturated to oven-dry [24], it was extremely important to correct for the "solution resistance" in the polarization resistance measurements. Traditional methods for correcting solution resistance, such as the current interrupt technique, could not be used since we could not get reliable readings from a reference electrode. Instead, we measured the resistance of the wooden block alone, immediately prior to the polarization resistance measurement and subtracted this from the measured polarization resistance. To do this, we replaced the working electrode with a second 25 mm cube of (inert) graphite and polarized the wood from −3 mV to +3 mV at a scan rate of 0.167 mV s^{-1}; the slope of this curve at the origin was the solution resistance. We chose this method because it has the same geometry and scan rate as the full polarization test, and the solution resistance could be calculated in the same way as the polarization resistance, except that there was (assumedly) no chemical reaction in the test with the two graphite electrodes. We present example

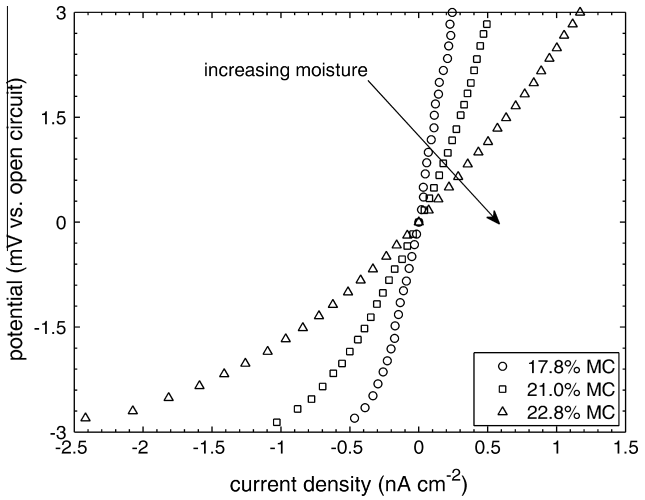

Fig. 3. Example polarization curves with two inert, graphite electrodes used to calculate the solution resistance of the wood. As the wood moisture content increased, the slope decreased. This slope was subtracted from the polarization resistance curve to correct for the effect of the high resistance of the wood.

data showing how the solution resistance was calculated in Fig. 3 which shows the potential vs. current density curves for wood at several different moisture contents. At higher moisture contents, the slope was lower, indicating a lower solution resistance. This slope, the solution resistance, was subtracted from the polarization resistance curve, with one metal and one graphite electrode, resulting in a corrected polarization resistance.

For dry (<15% MC) specimens, the total resistance was between 64 and 64,000 kΩ cm^2 (10 and 1000 kΩ) and the polarization resistances were greater than 64 kΩ cm^2. For the highest hygroscopic moisture contents, and all of the overhygroscopic and saturated specimens, the total resistance (solution + polarization) was less than 64 kΩ cm^2 and the measured solution resistances were around 6 kΩ cm^2 (1 kΩ) with a high amount of scatter in the data. The scatter results from uneven moisture distribution in the wood. In these cases, both the corrosivity of the wood and the solution resistance of wood are affected by areas of high moisture content, yet the measurements average over the entire surface area. For these specimens subtracting the solution resistance caused some of the measurements to have unreasonably high apparent corrosion rates. Therefore, for consistency between measurements, no correction was applied when the total measured resistance was less than 64 kΩ cm^2 (10 kΩ).

In preliminary testing, electrochemical impedance spectroscopy (EIS) was used as a complementary technique to the polarization resistance testing. However, in the preliminary testing, spectra collected at similar moisture contents exhibited different number of time constants, with no apparent systematic changes with the experimental variables. Therefore, EIS was not performed on all specimens, and data are not included in this paper.

All blocks were brought to the testing moisture content from an oven dry state (adsorption). The moisture content of the blocks was controlled by one of three techniques depending on the moisture regime. For the hygroscopic (below fiber saturation) region, the blocks were equilibrated for several weeks in small jars over saturated salt solutions, or glycerol–water solutions resulting in known RH in the air. The overhygroscopic (above fiber saturation but below full saturation) regime is not an equilibrium condition, making it difficult to attain a uniform moisture distribution or a specific moisture content. In this case, a pipette was used to deliver targeted amounts of water to each block to give a range of moisture contents. The blocks were then sealed in a polyethylene bag overnight so that the water could redistribute prior to testing. Despite this, the water appeared unevenly distributed (i.e. contained wet spots) upon visual inspection. The reason for the uneven water distribution is that the activity of the free water is the same throughout the specimen so there is no thermodynamic driving force for an even distribution of water. The third condition intended to test water-saturated samples, or the highest end of the overhygroscopic region. These samples were vacuum saturated by placing the samples underwater and pulling a vacuum to an absolute pressure 6 kPa (−95 kPa gauge pressure) for 30 min. The saturated specimens appeared to have a more uniform distribution of moisture since they could not physically hold any more water and all of the pores were filled with water.

3. Results

3.1. Gravimetric data

The corrosion rate as a function of moisture content for steel and galvanized fasteners is shown in Fig. 4 with the fit of Eq. (1) overlaid. The fit was obtained using the "Trust Region" curve fitting routines in Matlab™ (Natick, Massachusetts) with equal weights on all data points; nine data points were included at (0,0) to give it the same weight as the other conditions tested. The point at (0,0) was added as occasionally fits would give non-zero corrosion at zero moisture content. Previous studies have all shown that the corrosion rate becomes too low to be measureable between 12% and 15% MC [18–23]. Because of the shape of the function used, setting (0,0) results in the fit being nearly zero in the 12–15% range without specifying where the exact zero is and also prevents the data from exhibiting non-zero corrosion at zero moisture content. If anything, setting (0,0) is a slightly more conservative prediction tool than forcing zero at a higher moisture content.

The fit parameters and correlation coefficient are listed in Table 1 for reference. The galvanized steel curve shows a sharp increase in the corrosion rate as the moisture content increases from 0.2 to 0.3 with the corrosion rate remaining constant at the saturated condition. The steel data also shows an increase from 0.2 to 0.3 but the saturated data exhibited a lower corrosion rate than those measured in equilibrium with 100% relative humidity. Both curves can be captured by Eq. (1).

It is interesting that the steel fasteners exposed to saturated wood exhibited a lower corrosion rate than those embedded in

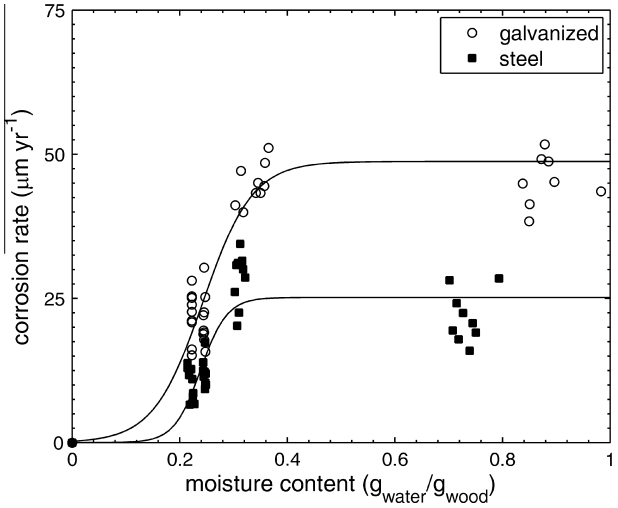

Fig. 4. Gravimetrically determined corrosion rates of steel and galvanized steel fasteners in ACQ-treated wood as a function of moisture content; note that the steel fasteners in the saturated condition exhibited a different corrosion mechanism involving cupric ions from the preservative plating on the fastener.

Table 1
Model (Eq. (1)) fit parameters and the corresponding goodness of fit statistics for various datasets.

Data set	A (μm/year)	B (g_{wood}/g_{water})	C (g_{water}/g_{wood})	R^2
Steel (gravimetric)	25.2	40.8	0.239	0.82
Galvanized (gravimetric)	48.8	21.8	0.243	0.92
Galvanized (electrochemical, hygroscopic and saturated conditions)	63.0	39.8	0.222	0.93
Galvanized (combined gravimetric and electrochemical hygroscopic and saturated conditions)	54.6	19.9	0.256	0.90

wood conditioned at 100% relative humidity. One possibility is that the corrosion mechanism was different in the saturated condition, and this change in corrosion mechanism is supported by observations of the corrosion products.

The steel fasteners exposed to the saturated condition exhibited several characteristics not seen for steel fasteners in any of the other moisture conditions and not seen at all for galvanized fasteners. A thin plating of copper appeared on the surface, likely deposited out from the wood preservatives (Fig. 5). Energy dispersive X-ray spectroscopy (EDS) measurements on the surface of the fasteners and powder X-ray diffraction patterns of the corrosion products confirmed that this deposit was indeed copper. Another difference in mechanism between the 100% RH and saturated conditions was the presence of pitting corrosion in the saturated condition (Fig. 5). The pitting occurred directly adjacent to the copper deposits. The steel fasteners exposed to the saturated condition were the only group to exhibit the copper plating or the pitting corrosion, and all steel fasteners exposed to the saturated condition exhibited both pitting corrosion and copper deposition.

The data are consistent with the function proposed by Zelinka et al. [25] and used in a combined hygrothermal corrosion model. It should be noted that the use of a continuous function for the steel fastener may be questionable since the corrosion mechanism changes between the 100% RH and saturated conditions. However, the function still adequately fits the data, as evidenced by its high R^2 value (0.82). It is uncertain if the change in corrosion mechanism of steel fasteners would occur if the wood were only saturated for short periods of time, as will occur in field exposures. If the corrosion mechanism did not change during short periods of saturation, Eq. (1) could still be used to analyze the results of hygrothermal simulations.

3.2. Corrosion product identification

The results of the X-ray diffraction experiments are summarized in Figs. 6 and 7. For the galvanized fasteners, the patterns

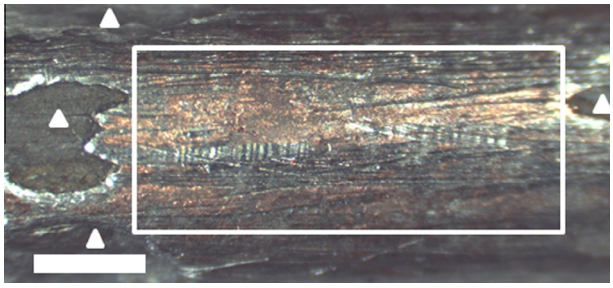

Fig. 5. Micrograph of a steel fastener exposed to water saturated wood, showing copper deposition and pitting corrosion. The triangles mark the location of the pits and the rectangle highlights a region of copper deposition. The scale marker represents 1 mm.

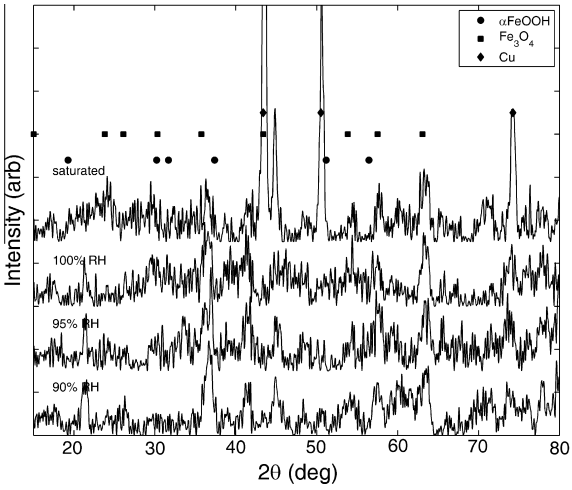

Fig. 6. Powder XRD patterns for the steel fastener corrosion products at different moisture conditions. The sharp peaks in the saturated condition are consistent with the pattern of copper.

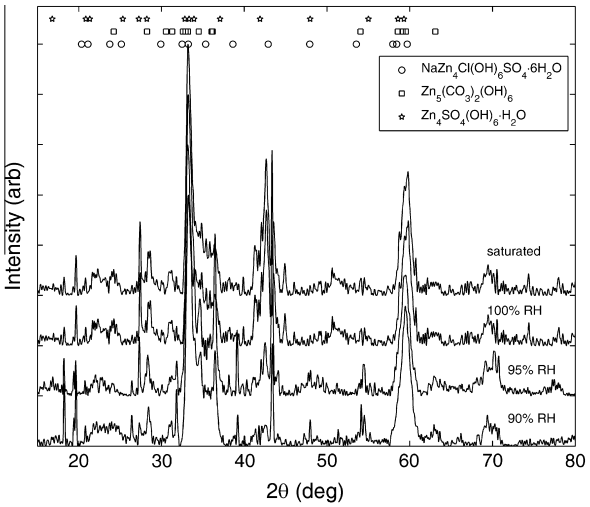

Fig. 7. Powder XRD patterns for the galvanized steel fastener corrosion products at different moisture conditions.

are similar over all moisture contents, suggesting that the corrosion products are composed of the same phases regardless of the moisture content. Some of the smaller peaks appear to have an increase or decrease in relative intensity across moisture contents, which suggests that the relative amounts of a given phase may change slightly with wood moisture content. Similarly, the steel fasteners have the same peaks as the moisture content is changed, with the notable exception of the steel fasteners exposed to the saturated wood. In this case, there are clear, well defined peaks that correspond with the powder XRD pattern of copper metal. It is clear from the XRD pattern that the copper-colored deposit in Fig. 4 is copper metal and that this phase is not present in any of the other conditions tested.

The specific crystalline phases present in the corrosion products are indicated by labeling the major peaks in Figs. 6 and 7. For the steel fasteners, the major phases that were observed were goethite (α-FeOOH) and magnetite (Fe_3O_4), with the exception of the saturated condition, which also contained copper metal. While the peaks were more intense in the galvanized steel corrosion products, the phases did not match as well. It appears that the corrosion products contain namuwite ($Zn_4SO_4(OH)_6{\cdot}H_2O$), and possibly

hydrozincite ($Zn_5(CO_3)_2(OH)_6$) and zinc chlorohydroxysulfate ($NaZn_4Cl(OH)_6SO_4{\cdot}6H_2O$). With the exception of zinc chlorohydroxysulfate, these were the same phases identified by Zelinka et al. in a one year laboratory test of galvanized steel fasteners exposed at 100% relative humidity [27].

3.3. Electrochemical data

The corrosion rate data from the polarization resistance tests for galvanized steel are shown in Fig. 8. The hygroscopic, over-hygroscopic, and saturated results are given different markings for clarity. The data are plotted with the same *x*-axis scale as Fig. 4 for easy comparison.

For the hygroscopic and saturated specimens the water was evenly distributed within the wood. Electrochemical measurements of the corrosion rate on these specimens were consistent with the gravimetric data. We overlay the gravimetric data and electrochemical data (from the hygroscopic and saturated groups) in Fig. 9 along with a global curve fit of both types of measurements. The fit parameters of the global fit (Eq. (1) and Table 1), with the exception of *B*, were within 30% of the parameters for the independent fits to gravimetric and electrochemical data, and the model fit the combined data with a high R^2 (0.90). Previous sensitivity analyses showed that the simulated corrosion is the least sensitive to *B* [25].

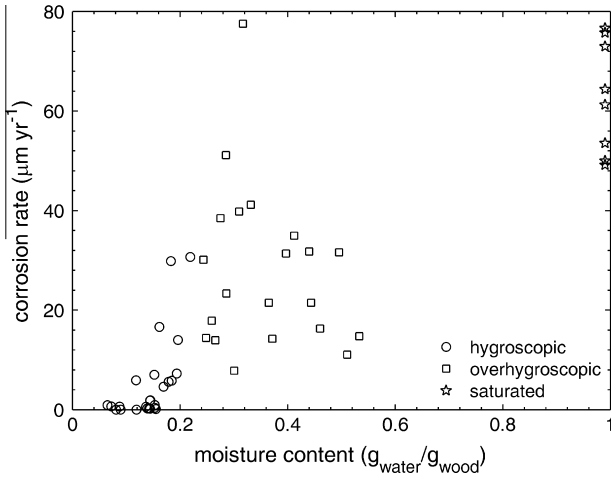

Fig. 8. Electrochemically determined corrosion rate of galvanized steel as calculated from polarization resistance measurements. Note that the data at the saturated condition were shifted to a moisture content of 0.99 g/g so that the data could be plotted on the same scale as Figs. 3 and 4. Actual moisture contents ranged from 1.07 to 1.80 g/g.

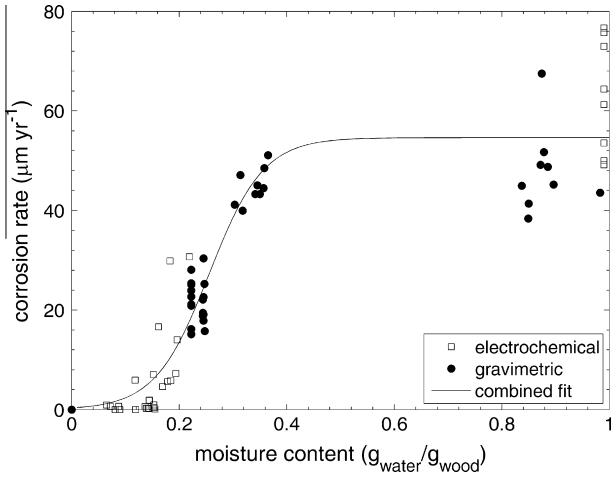

Fig. 9. Corrosion rate of galvanized steel measured electrochemically and gravimetrically with a curve fit of the combined data set overlayed. Note that the data at the saturated condition were shifted to a moisture content of 0.99 g/g so that the data could be plotted on the same scale as Figs. 3 and 4. Actual moisture contents ranged from 1.07 to 1.80 g/g.

The data from the overhygroscopic region contain a lot of scatter (Fig. 8). During testing, it was observed that the specimens in the overhygroscopic region did not have an even distribution of water, with some spots visually appearing much wetter than others. The reported moisture content in Fig. 8 represents the average moisture content over the entire volume of the wood block. Likewise, the corrosion rate is based upon the measured current divided by the entire area of the electrode. These data are likely so noisy because the current was dominated by the saturated areas of wood in contact with the electrode and then averaged over the entire area. While the corrosion rate appears to be an increase between the specimens in the overhygroscopic region and the saturation condition, the difference in Fig. 8 appears larger than it may actually be since there is a 100% increase in moisture between the overhygroscopic and saturated specimens and also the highest overhygroscopic measurements had low corrosion rates, assumedly because of unequal moisture distribution in the wood.

4. Discussion

Wood moisture content greatly affects the corrosion rate of embedded metal fasteners. The goal of this work was to precisely characterize the dependence of the corrosion rate on the moisture content, and both electrochemical and gravimetric methods were used. Unlike previous work that had examined the relationship between corrosion and moisture content only below fiber saturation, data were collected over a broad range of moisture contents from dry (7% MC) to fully saturated with water. The data were consistent with a previous model used to fit the dependence of the corrosion rate on the wood moisture content. The discussion herein is based upon our measurements of ACQ-treated southern pine; different wood species or treatments may behave differently.

Despite the agreement of the current data with the model, the reliability of the model could be further improved by even more precise data over the range of moisture contents. The most striking challenge is to measure the corrosion rate in the overhygroscopic regime. Whereas vapor water distribute very uniformly in wood, liquid water does not do so. Once the cell walls are hygroscopically full, the liquid water resides only in the pore systems. Capillary action leads water in the finer pores (typically lumina of latewood). Because wood consists of a complex network of lumina of different sizes, it is extremely difficult to add liquid water in a uniform manner in the overhygroscopic region. The saturated condition was an exception, as all lumina were and other pores were filled to the maximum amount, making a uniform distribution of liquid water.

The ability to obtain accurate and precise data over the range of wood moisture contents is limited by inherent experimental difficulties in both the electrochemical and gravimetric measurements. The exposure tests require the samples to remain at a constant moisture content for an entire year, which limits the moisture contents that can be tested to the hygroscopic and saturated regions, and is further limited by the difficulty in maintaining a constant relative humidity for long times.

While in theory the rapidity of electrochemical measurements should allow the whole range of moisture contents to be tested in a reasonable amount of time, the experiments were limited not only by the difficulty of equilibrating specimens in the overhygroscopic region, but also because of inherent difficulties in

attempting to apply electrochemical techniques to a poorly conducting solid electrolyte. Because wood is a porous solid that has complex interactions with water, it was impossible to get reliable and repeatable readings from a reference electrode. The lack of a reference electrode precluded an accurate correction for solution resistance by the current-interrupt technique and instead required the solution resistance to be measured in a separate test. While this method of correction for the solution resistance appeared to have worked in some cases, it was unsuitable for when the total resistance was less than 64 $k\Omega\,cm^2$. Future work in this area would require a better method for determining and correcting for the solution resistance. Beyond the complications in the electrochemical testing itself, condition the overhygroscopic specimens resulted in an uneven distribution of moisture, which introduced a considerable amount of scatter into the data. The result of these experimental limitations was that it was impossible to measure the corrosion rate directly above the fiber saturation point, which was an important part of the curve.

The agreement between the electrochemical and gravimetric measurements is notable given the differences in the measurement techniques. The electrochemical measurements represent an instantaneous determination of a corrosion rate, whereas the exposure test represents the average corrosion rate over 1 year at a constant environmental condition. Zelinka et al. observed agreement between corrosion rates measured in an electrochemical test using a water extract of wood and in an exposure test using solid wood [29]. They concluded that corrosion of metals in solid wood is activation controlled (that is, it depends on the electron transfer reaction at the metal surface and not diffusion of ions to the surface) and that the corrosion rate does not decrease with time. Other work has shown that the corrosion rate of fasteners embedded in wood is constant with time from 6 months to 17 years [28,41]. Furthermore, the self-diffusion rate of copper in wood is able to support a corrosion rate of over 60 $\mu m\,year^{-1}$, given the initial copper concentration of 1.9 $kg\,m^{-3}$ [42]. The measurements presented here are consistent with these observations of an activation controlled reaction. The consistency between instantaneous electrochemical measurements and long-term exposure tests supports the assertion that the corrosion rate (as a function of moisture content) is constant with time in wood and further justifies the use of a corrosion post-processor for hygrothermal models that does not require previous history as an input.

One unexplained result is why the steel fastener exhibited a change in mechanism in the saturated condition. The mechanism of corrosion in treated wood involves the reduction of cupric ions, and therefore we would expect reduced copper (copper metal) to appear on the fasteners in all situations. In fact we observed nearly the opposite. For wood at lower moisture contents, no copper plating was observed, even though the most probably cathodic reaction was the reduction of cupric ions in the wood. These results agree with the results of similar studies of steel and galvanized steel in treated wood where the reduction of cupric ions was identified as the cathodic reaction, yet no deposited copper was found on the fasteners [27]. At these lower moisture contents, it is unclear what happens to the reduced copper. The copper plating observed on the fasteners exposed to the saturated condition agrees with observations from testing in dilute solutions of wood preservatives and electrochemical testing in water extracts of treated wood where copper is deposited on the metal surface [29,43–46]. Therefore, it appears that free water is necessary for the copper deposition part of the corrosion reaction. However, it is unclear why copper deposition did not occur on the galvanized fasteners in the saturated condition, since they were in wood at a similar moisture content as the steel fasteners, and the thermodynamics favor cupric ion reduction. Further work is needed to determine what happens to the cupric ions in the other moisture conditions. One possibility would be to examine cupric ion diffusion and accumulation using micro X-ray fluorescence spectroscopy.

One of the reasons for conducting the investigation was to further develop previous work where combined hygrothermal–corrosion models for wood were developed using limited data. Thus, refining the data used in the post-processor is a main output of the present work. It is instructive to examine the data obtained in light of the improvement it has provided and also what data would need to be obtained for predicting corrosion in different wood species or treatments. The original post-processor was based upon polarization resistance measurements in CCA-treated wood that were proportionally scaled to measured data of hot-dip galvanized steel in ACQ-treated wood; this implicitly assumed that the parameters B and C remained roughly the same and that they did not largely affect the simulated corrosion [25]. We found B to be within the range of 20–40 and C to range from 0.22 to 0.25 (Table 1); the original post-processor had $B = 80$ and $C = 0.24$. Zelinka et al. analyzed the sensitivity of simulated corrosion to the model fit parameters B and C [25]. Corrosion was most sensitive to C, which is related to the threshold moisture content at which corrosion begins, and doubled as C was decreased from a moisture content of 0.24 to 0.14 g/g. The present measurements are close to the original value of 0.24 g/g. The parameter B, physically the steepness of the transition, had much less of an effect on the simulated corrosion, but the parameter B obtained by fitting the current data is appreciably lower than the original value of 80 (obtained by fitting the data of Dennis et al. [22]. Based upon the previous sensitivity analysis the difference in corrosion between $B = 20$ and $B = 80$ should be less than 25%. Comparing the fit parameters in this work, which comprised steel and hot-dip galvanized steel in ACQ-treated wood with those from Zelinka et al. which were effectively of hot-dip galvanized steel in CCA-treated wood suggest that the differences in parameters B and C result in small changes in the simulated amount of corrosion. Since the parameter A represents the maximum corrosion rate, which is much easier to measure than the entire curve, it may be possible to extend the corrosion model to other fasteners and preservative treatments by measuring only the maximum corrosion rate and using the existing parameters B and C in the absence of better data.

5. Conclusions

Corrosion rates were measured gravimetrically in 1 year exposures tests for steel and hot-dip galvanized steel nails embedded in ACQ-treated wood conditioned at several different moisture contents. Additional electrochemical measurements were performed at many different moisture contents for hot-dip galvanized steel coupons.

The gravimetric corrosion data were consistent with a previously used model for the dependence of the corrosion rate on the wood moisture content.

The steel fasteners exhibited a change in the corrosion mechanism when exposed to moisture saturated wood. Copper from the wood preservative was deposited on the surface. It is unclear why this only happened for the steel fasteners; furthermore, it is unclear under which moisture conditions this change in mechanism occurs.

The X-ray diffraction patterns for corrosion products were similar across all moisture contents and also similar to those measured previously in treated wood. Steel fasteners formed goethite (α-FeOOH) and magnetite (Fe_3O_4); the galvanized fasteners formed namuwite ($Zn_4SO_4(OH)_6{\cdot}H2O$), and possibly hydrozincite ($Zn_5(CO_3)_2(OH)_6$) and zinc chlorohydroxysulfate ($NaZn_4Cl(OH)_6SO_4{\cdot}6H_2O$).

The electrochemical measurements provided more data and were generally consistent with the exposure data except in the

overhygroscopic range, where samples had a non-uniform distribution of moisture. The samples conditioned either by equilibrating over saturated salt solutions or by vacuum-saturation with water were in alignment with the gravimetric data. This agreement between the instantaneous electrochemical tests and one-year exposure tests is consistent with previous data that shows that the corrosion rate of embedded metals is constant with time.

The model fit parameters B and C, which describe the midpoint and steepness of the corrosion rate versus moisture content curve, were similar for exposure tests and electrochemical tests and were similar to those in the original corrosion post-processor. For processing data in a new wood treatment, it may be sufficient to only measure the maximum corrosion rate (parameter A) and use existing values of B and C to estimate the dependence of corrosion on the wood moisture content.

References

[1] C.A. Smith, Corrosion of metals by wood, Anti-Corros. Methods Mater. 29 (1982) 16–17.
[2] C.A. Smith, Acid vapour from wood can damage metal fastenings, Tim. Trades J. 313 (1980). pp. 27–27.
[3] A.J. Baker, Corrosion of metal in wood products, in: Durability of Building Materials and Components, ASTM STP 691, American Society for Testing and Materials, West Conshohocken, PA, 1980, pp. 981–993.
[4] J.N. Cross, Evaluation of metal fastener performance in CCA treated timber, in: J.M. Baker (Ed.), E & FN Spon, London, 1990.
[5] R.H. Falk, A.J. Baker, Fasteners for exposed wood structures, Wood Des. Focus 4 (1993) 14–17.
[6] G. Kear, M.S. Jones, P. Haberecht, Corrosion of mild steel, HDG steel, and 316 stainless steel in CCA, CuAz and ACQ-treated Pinus radiata, Beijing, China, 2005.
[7] G. Kear, M.S. Jones, P.W. Haberecht, Corrosion of mild steel HDG steel and 316 stainless steel in CCA CuAz and ACQ treated Pinus radiata, Gold Coast, Australia, 2005.
[8] G. Kear, H.Z. Wú, E.W. Bruce, C. Kane, M.S. Jones, Metallic materials selection for timbers treated with non-CCA-based, copper-rich preservatives: implications for Australasia, Corros. Mater. 32 (2007) 16–21.
[9] G. Kear, H.Z. Wú, M.S. Jones, The corrosion of metallic fastener materials in untreated, CCA-, CuAz0 and ACQ-based timbers, BRANZ, Porirua City, New Zealand, 2006, pp. 281–281.
[10] G. Kear, H.Z. Wú, M.S. Jones, Non-accelerated weight loss studies of fastener material corrosion in contact with CCA, CuAz, and ACQ-treated timbers, Hobart Australia, 2006.
[11] G. Kear, H.-Z. Wu, M.S. Jones, Weight loss studies of fastener materials corrosion in contact with timbers treated with copper azole and alkaline copper quaternary compounds, Corros. Sci. 51 (2009) 252–262.
[12] Z. Li, Corrosion of fasteners, Build (2009) 47–48.
[13] D.W. Simm, H.E. Button, Electrochemical measurements on metals in CCA-treated wood, Corros. Prevent. Contr. 32 (1985) 67–74. 83–67–74, 83.
[14] D.W. Simm, H.E. Button, Corrosion behaviour of certain materials in CCA-treated timber. Environmental tests at 100% relative humidity, Corros. Prevent. Contr. 32 (1985) 25–35.
[15] R.H. Farmer, Corrosion of metals in association with wood. Part 2. Corrosion of metals in contact with wood, Wood 27 (1962) 443–446.
[16] R.H. Farmer, R.C. Porter, The corrosion of metals in association with wood. Pt. 3: corrosion of aluminum in contact with wood, Wood 28 (1962) 505–507.
[17] R.A. Laidlaw, R.N. Cox, The effect of preservatives on the corrosion of galvanized metal plate fasteners in timber. Pt. 1, Effect of joint strength and the significance for trussed rafter roofs, The International Journal of Wood Preservation, vol. 3, pp. 51–60.
[18] A.J. Baker, Corrosion of metals in preservative-treated wood, in: M. Hamel (Ed.), Wood Protection Techniques and the Use of Treated Wood in Construction, Forest Products Society, Madison, Wisconsin, 1988, pp. 99–101.
[19] R.H. Baechler, Corrosion of metal fastenings in zinc-chloride treated wood after ten years, in: Proceedings of the 35th Annual Meeting of the American Wood Preservers' Association, Washington, D.C., 1939, pp. 56–63.
[20] R.H. Baechler, Corrosion of metal fastenings in zinc-chloride treated wood after 20 years, in: Proceedings of the 45th Annual Meeting of the American Wood Preservers' Association, American Wood Preservers' Association, St. Louis, MO, 1949, pp. 381–397.
[21] S.L. Zelinka, D.R. Rammer, Synthesis of published and unpublished corrosion data from long term tests of fasteners embedded in wood: calculation of corrosion rates and the effect of corrosion on lateral joint strength, in: CORROSION 2011, NACE International, Houston, TX, 2011, Paper No. 11163.
[22] J.K. Dennis, C. Zou, N.R. Short, Corrosion behaviour of zinc and zinc alloy coated steel in preservative treated timber, Trans. Inst. Met. Finish. 75 (1995) 96–101.
[23] N.R. Short, J.K. Dennis, Corrosion resistance of zinc-alloy coated steel in construction industry environments, Trans. Inst. Met. Finish. 75 (1997) 47–52.
[24] S.V. Glass, S.L. Zelinka, Moisture relations and physical properties of wood, in: R.J. Ross (Ed.), Wood Handbook, Wood as an Engineering Material, U.S. Department of Agriculture, Forest Service, Forest Products Laboratory, 2010.
[25] S.L. Zelinka, D. Derome, S.V. Glass, Combining hygrothermal and corrosion models to predict corrosion of metal fasteners embedded in wood, Build. Environ. 46 (2011) 2060–2068.
[26] S.L. Zelinka, D.S. Stone, Corrosion of metals in wood: comparing the results of a rapid test method with long-term exposure tests across six wood treatments, Corros. Sci. 53 (2011) 1708–1714.
[27] S.L. Zelinka, R.J. Sichel, D.S. Stone, Exposure testing of fasteners in preservative treated wood: gravimetric corrosion rates and corrosion product analyses, Corros. Sci. 52 (2010) 3943–3948.
[28] S.L. Zelinka, D.R. Rammer, Corrosion rates of fasteners in treated wood exposed to 100% relative humidity, ASCE J. Mater. Civ. Eng. 21 (2009) 758–763.
[29] S.L. Zelinka, D.R. Rammer, D.S. Stone, Electrochemical corrosion testing of fasteners in wood extract, Corros. Sci. 50 (2008) 1251–1257.
[30] X.G. Zhang, Corrosion of zinc and zinc alloys, in: S.D. Cramer, B.S. Covino (Eds.), ASM Handbook, Corrosion: Materials, vol. 13B, ASM International, Materials Park, OH, 2003, pp. 402–417.
[31] X.G. Zhang, J. Hwang, W.K. Wu, Corrosion testing of steel and zinc, in: Proceedings of the 4th International Conference on Zinc and Zinc Alloy Coated Steel Sheet (GALVATECH '98), Chiba, Japan, 1998.
[32] Anon, ASTM G198–11: Standard Test Method for Determining the Relative Corrosion Performance of Driven Fasteners in Contact with Treated Wood, ASTM International, West Conshohocken, PA, 2011.
[33] Anon, AWPA P5: Standard for waterborne preservatives, American Wood Preservers' Association, Granbury, TX, 2007.
[34] Anon, AWPA U1–06: Use category system, American Wood Preservers' Association, Granbury, TX, 2007.
[35] D.R. Rammer, S.L. Zelinka, Optical method for measuring the surface area of a threaded fastener, Exp. Tech. 34 (2010) 36–39.
[36] D.R. Rammer, S.L. Zelinka, Algorithm to calculate the surface area of a threaded fastener, United States Patent No. 8,041,150, 2011.
[37] D.R. Rammer, S.L. Zelinka, Analytical determination of the surface area of a threaded fastener, ASTM J. Test. Eval. 36 (2008) 80–88.
[38] S.L. Zelinka, D.S. Stone, D.R. Rammer, Equivalent circuit modeling of wood at 12% moisture content, Wood Fiber Sci. 39 (2007) 556–565.
[39] F. Mansfeld, Simultaneous determination of instantaneous corrosion rates and Tafel slopes from polarization resistance measurements, J. Electrochem. Soc. 120 (1973) 515–518.
[40] F. Mansfeld, Tafel slopes and corrosion rates from polarization resistance measurements, Corrosion 29 (1973) 397–402.
[41] A.J. Baker, Corrosion of nails in CCA- and ACA-treated wood in two environments, Forest Prod. J. 42 (1992) 39–41.
[42] S. Zelinka, Corrosion of embedded metals in wood: an overview of recent research with implications for building moisture design, ASHRAE Trans. 119 (2013) 442–449.
[43] S.L. Zelinka, D.R. Rammer, D.S. Stone, J.T. Gilbertson, Direct current testing to measure corrosiveness of wood preservatives, Corros. Sci. 49 (2007) 1673–1685.
[44] G. Kear, H. Wú, M.S. Jones, F.C. Walsh, Direct-current methods for the estimation of corrosion rates in aqueous timber preservatives, Aust. J. Chem. 61 (2008) 455–465.
[45] G. Kear, H.Z. Wú, M.S. Jones, Corrosion of ferrous- and zinc-based materials in CCA, ACQ, and CuAz timber preservative solutions, Mater. Struct. 41 (2008) 1405–1417.
[46] G. Kear, H.-Z. Wu, M.S. Jones, F. Walsh, Impedance spectroscopy studies of the dissolution of ferrous- and zinc-based materials in aqueous timber preservatives, J. Appl. Electrochem. 38 (2008) 1599–1607.